Homogeneous precipitation of layered Ni(II)–Cr(III) double hydroxides

Matías Jobbágy [a], Miguel A. Blesa [b,c], Alberto E. Regazzoni [b,d,*]

[a] INQUIMAE, Facultad de Ciencias Exactas y Naturales, Universidad de Buenos Aires, Pabellón II, Ciudad Universitaria, C1428EHA Buenos Aires, Argentina
[b] Unidad de Actividad Química, Centro Atómico Constituyentes, Comisión Nacional de Energía Atómica, Av. General Paz 1499, B1650KNA San Martín, Argentina
[c] Escuela de Posgrado, Universidad Nacional de General San Martín, Av. General Paz 1499, B1650KNA San Martín, Argentina
[d] Instituto de Tecnología Jorge Sábato, Universidad Nacional de General San Martín, Av. General Paz 1499, B1650KNA San Martín, Argentina

Abstract

An adequate account of the hydrolytic properties of Cr^{3+} and Ni^{2+} allows setting the conditions for homogeneous nucleation of layered Ni(II)–Cr(III) double hydroxides; water exchange and hydrolysis rate constants indicate that, at very high rates of base dosing, formation of heteronuclear Cr(III)–Ni(II) hydroxo species should prevail over precipitation of active $Cr(OH)_3$. This is realized by the urea method under microwave-assisted hydrothermal conditions. This approach yields crystalline $Ni_{1-x}Cr_x(OH)_2(CO_3)_{x/2} \cdot nH_2O$ ($x \approx 0.32$–0.36) in less than 5 min at 453 K; higher degrees of crystallinity are obtained at higher temperatures and/or longer aging times. Formation of Ni(II)–Cr(III) LDHs upon microwave-assisted hydrothermal aging of freshly coprecipitated $Ni(OH)_2 + Cr(OH)_3$ mixtures takes longer, due to a different operating mechanism. The implications of the advanced rationale for the design of synthesis procedures are stressed. It is proposed that homogeneous nucleation of Ni(II)–Cr(III) LDHs involves the edge-on condensation of planar heteronuclear Cr(III)–Ni(II) hydroxo trimers. Ordered aggregation of primary particles leads to the final platelet crystals, a process that involves the exchange of CO_3^{2-} ions dangling at the crystallites' edges by bridging OH^-.
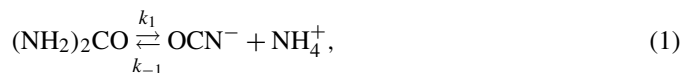© 2007 Elsevier Inc. All rights reserved.

Keywords: Layered double hydroxides; Hydrotalcites; Homogeneous precipitation; Nickel hydroxide; Chromium hydroxide

1. Introduction

Layered double hydroxides (LDHs), also known as *anionic clays*, constitute a large family of compounds with general formula $M(II)_{1-x}M(III)_x(OH)_2A_{x/m} \cdot nH_2O$, x varying within the approximate limits 0.15 and 0.36. They are stacks of partially substituted brucite-like sheets in which the A^{m-} anions and water molecules occupy the interlamellar space. The increasing interest for these materials arises from their use as catalyst precursors and catalyst supports, including heterogeneous catalysis in liquid media, as precursors for mixed oxides, as inorganic exchangers, and as vehicles for the preparation of hybrid materials and a huge variety of intercalation compounds [1–3].

The growing attention devoted to LDH-based materials has prompted the search for simpler, less time-consuming, and reliable synthesis procedures leading to LDH particles of con-

trolled chemical composition, crystallinity, and textural characteristics. Typically, LDHs are synthesized following with slight modifications the recipe advanced by Miyata and Okada [4], i.e., coprecipitation followed by aging at moderate temperatures; the length of the aging stage depends on the degree of crystallinity that is pursued [5] and can be shortened by microwave dielectric heating [6–8]. Recently, LDH particles have also been prepared via the urea method [9–12], in which the rate of homogeneous alkalization is determined by the rate of urea hydrolysis [13],

$$(NH_2)_2CO \underset{k_{-1}}{\overset{k_1}{\rightleftharpoons}} OCN^- + NH_4^+, \tag{1}$$

$$OCN^- + 2H_2O \overset{k_2}{\to} HCO_3^- + NH_3. \tag{2}$$

Contrasting with the abundant literature referring to the synthesis and properties of many different M(II)–M(III) LDHs, the information on Ni(II)–Cr(III) LDHs, which have been envisaged as potential electrode materials for alkaline secondary cells [14], is indeed scarce. The preparation of crystalline

Ni(II)–Cr(III) LDHs requires rather stringent conditions, i.e., prolonged hydrothermal aging of coprecipitated $Ni(OH)_2$ + $Cr(OH)_3$ mixtures (48 h at 470 K [5] or 11 days at 400 K [15]). In spite of a previous claim [16], coprecipitation from Ni(II) and Cr(III) salt solutions at room temperature leads to X-ray amorphous solids [14,17]. In addition, under the usual synthesis conditions the urea method proved inadequate for the preparation of Cr(III)-containing LDHs [9].

Clearly, the difficult synthesis of crystalline Ni(II)–Cr(III) LDHs is a consequence of the sluggish substitution kinetics of the inert d^3 Cr(III) and d^8 Ni(II) ions. In the present paper we show that this liability can be overcome once the basic principles of coordination chemistry are adequately considered and report the fast synthesis of crystalline Ni(II)–Cr(III) LDHs by the urea method under microwave-assisted hydrothermal conditions. Hydrothermal conditions lead to increased rates of water exchange in the hexaaquo Ni^{2+} and Cr^{3+} ions and of urea hydrolysis. The use of a microwave reactor further grants fast heating with minimum temperature gradients, allowing a rapid and homogeneous rise of the driving force for precipitation.

2. Experimental

Layered Ni(II)–Cr(III) hydroxides were synthesized by aging $Ni(NO_3)_2$–$Cr(NO_3)_3$–urea aqueous solutions for different periods at prefixed temperatures; aging periods spanned from 5 to 180 min, whereas temperature was varied between 413 and 493 K. A 600-W commercial Milestone microwave digester, fitted with pressure and temperature probes, was used in all experiments. Solutions were made up from analytical grade reagents; they were filtered through 0.22-µm pore-size cellulose nitrate membranes. The total metal concentration ($C_0 = [Ni(II)]_0 + [Cr(III)]_0$) was 0.04 or 0.01 M, whereas the chromium-to-total-metal mole ratio ($X_{Cr} = [Cr(III)]_0/C_0$) was 0.31 or 0.36. The concentration of urea was 0.5 M, and the initial pH, adjusted by the addition of HNO_3, was 3.0 ± 0.05.

In each run, a freshly prepared solution was poured into eight heavy-duty Teflon vessels, which were then sealed and placed in the microwave digester. The systems were then heated at maximum power output; the working temperature, which was kept constant within ± 3 K, was attained in less than 15 min, depending on the set value. After aging, the reaction vessels were immersed in a water bath until the pressure dropped to 0.1 MPa. The precipitates were then separated by centrifugation, washed thoroughly with water, and dried in vacuo at room temperature.

In a different set of experiments, nickel and chromium hydroxides were coprecipitated at room temperature by mixing stoichiometric amounts of NaOH and $NaHCO_3$ with 200 ml of a solution containing $Ni(NO_3)_2$ (0.026 M) and $Cr(NO_3)_3$ (0.012 M); the final pH was 10. The resulting suspensions were then aged in the microwave digester.

The synthesized solids were characterized by powder X-ray diffraction (PXRD) using graphite-filtered Cu$K\alpha$ radiation ($\lambda = 1.5406$ Å), Fourier-transform infrared spectroscopy (FTIR), electron microscopy (TEM and SEM), energy-dispersive spectroscopy (EDS), and electron diffraction. Diffractograms were collected at step size 0.01° and counting time

1 s. Peak analyses were performed using the Diffrac-AT 3.0 profile fitting software provided by Siemens (Karlsruhe, Germany, 1993). FWHM (full width at half maximum), from which crystallite sizes were derived using the Scherrer equation, was corrected for instrumental broadening; a crystalline quartz specimen was used as reference. Transmission FTIR spectra were recorded at resolution 0.5 cm^{-1} after 500 scans, using a MCT-A detector. For chemical analyses, the solids were dissolved in 1:1 HNO_3, and Ni(II) and Cr(III) were assayed by atomic absorption spectrometry. Elemental analyses were carried out in a Carlo Erba CHON-S analyzer. Supernatants were inspected for unreacted Ni(II) and Cr(III).

3. Results

Fig. 1 A–C show the PXRD patterns of the solids synthesized from $Ni(NO_3)_2$–$Cr(NO_3)_3$–urea solutions ($C_0 = 0.04$ M; $X_{Cr} = 0.31$) aged for 1 h at different temperatures. All patterns present reflections at d spacings that are typical of LDHs. The derived lattice parameters (hexagonal cell, space group R-$3m$), which are presented in Table 1, are in excellent agreement with those reported earlier [5,15]. As expected, crystallinity increases with temperature. Although pattern C does not exclude the presence of turbostratic α-Ni(OH)$_2$ and amorphous Cr(OH)$_3$, the FTIR spectrum of the sample (Fig. 2C) rules out this possibility; FTIR spectra of α-Ni(OH)$_2$ powders synthesized by the urea method are characterized by a sharp band

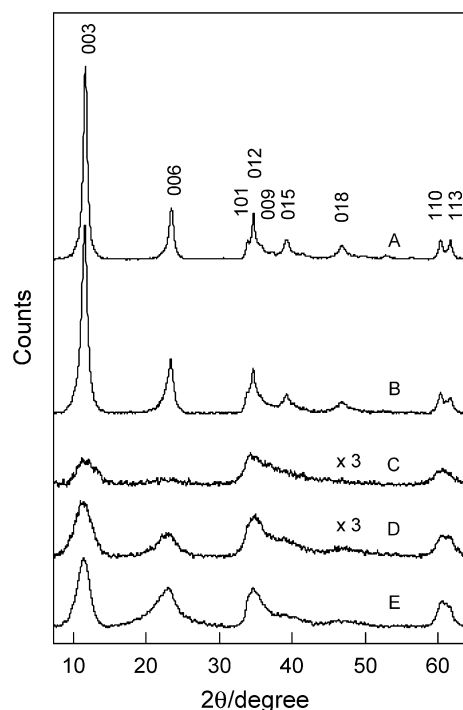Fig. 1. PXRD patterns of layered Ni(II)–Cr(III) hydroxides formed from $Ni(NO_3)_2$–$Cr(NO_3)_3$–urea solutions aged at 483 (A), 453 (B), and 413 K (C). Aging time 1 h; initial solution composition $C_0 = 0.04$ M; $X_{Cr} = 0.31$; urea = 0.5 M. Diffractogram D corresponds to a Ni(II)–Cr(III) LDH formed after the aging of freshly co-precipitated $Ni(OH)_2$–$Cr(OH)_3$; $T = 483$ K; aging time 1 h. Diffractogram E corresponds to the solid precipitated from $C_0 = 0.01$ M, $X_{Cr} = 0.36$, urea = 0.5 M solutions aged at 453 K for 5 min.

Table 1
Characteristics of Ni(II)–Cr(III) LDHs synthesized from Ni(NO$_3$)$_2$–Cr(NO$_3$)$_3$–urea solutions aged under microwave-assisted hydrothermal conditions for 1 h[a]

T (K)	a (nm)	c (nm)	L_{003} (nm)	L_{110} (nm)	x[b]	σ[c]	Cr/C
413	0.307(1)	2.32(2)	2.9(2)	6.0(3)	0.329	0.014	1.41
453	0.3068(2)	2.29(1)	9.6(4)	11.7(5)	0.313	0.012	1.86
483	0.3066(2)	2.28(1)	13.8(6)	16.2(7)	0.317	0.007	1.95
483[d]	0.306(1)	2.34(3)	3.6(2)	5.9(3)			

[a] $C_0 = 0.04$ M; $X_{Cr} = 0.31$; urea = 0.5 M.
[b] Determined by EDS.
[c] Standard deviation of EDS analyses.
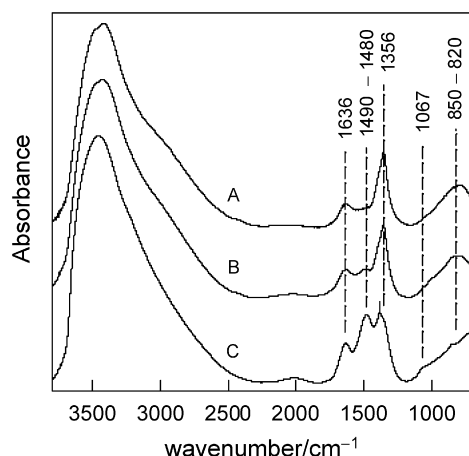[d] Prepared by microwave hydrothermal aging of a freshly coprecipitated Ni(OH)$_2$ + Cr(OH)$_3$ suspension.

Fig. 2. FTIR spectra of Ni(II)–Cr(III) LDHs formed from Ni(NO$_3$)$_2$–Cr(NO$_3$)$_3$–urea solutions aged at 483 (A), 453 (B), and 413 K (C). Aging time 1 h; initial solution composition $C_0 = 0.04$ M; $X_{Cr} = 0.31$; urea = 0.5 M.
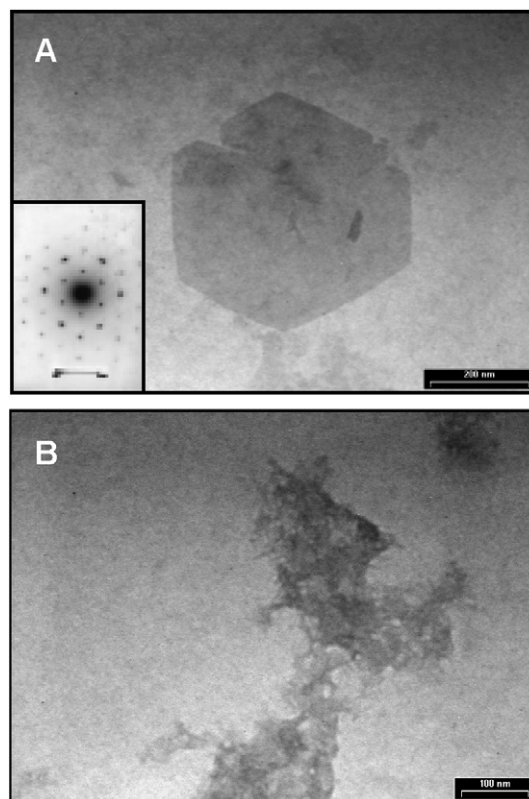

Fig. 3. TEM micrographs of Ni(II)–Cr(III) LDHs formed from $C_0 = 0.04$ M, $X_{Cr} = 0.31$, urea = 0.5 M solutions aged for 1 h at 483 (A) and 413 K (B). Markers correspond to 200 and 100 nm, respectively. The inset in A shows the electron diffraction pattern of the sample.

at ca. 3650 cm^{-1} due to the $\nu_{O–H}$ stretching of free geminal OH groups and a very intense one at ca. 2250 cm^{-1} due to the $\nu_{C\equiv N}$ stretching of coordinated isocyanate [18–20]. Thus, the diffractogram of the solid obtained at 413 K must be assigned to nanocrystalline Ni(II)–Cr(III) LDH.

Fig. 1D corresponds to the product obtained by aging freshly coprecipitated, X-ray amorphous, Ni(OH)$_2$ + Cr(OH)$_3$ mixtures for 1 h at 483 K. Comparison of Fig. 1 patterns A and D shows that the urea method alone produces well-crystallized Ni(II)–Cr(III) LDHs. Nevertheless, microwave-hydrothermal aging of coprecipitated Ni(OH)$_2$ + Cr(OH)$_3$ mixtures is also satisfactory. The benefits of microwave-hydrothermal treatments over conventional hydrothermal ones have already been discussed [21,22].

Fig. 2 shows the FTIR spectra of the solids prepared by the urea method. They are typical of carbonate-containing LDHs, including Ni$_{0.67}$Cr$_{0.33}$(OH)$_2$(CO$_3$)$_{0.165}$·nH$_2$O [5,15]. The broad band centered at ca. 3440 cm^{-1} is due to the $\nu_{O–H}$ stretching vibration of hydrogen-bonded geminal OH groups and water molecules, and that at 1636 cm^{-1} corresponds to the bending of water. The bands at 1356 and 820–850 cm^{-1} are due to the ν_3 asymmetric stretching and the out-of-plane deformation of free interlamellar carbonate ions (D_{3h} symme-

try), respectively. Those at 1480–1490, 1388 (shoulder), and 1067 cm^{-1} are also attributed to intercalated carbonate ions, but in the lower C_{2v} symmetry [23–26]. The sharp band at 1384 cm^{-1}, evident in spectrum C only, is due to intercalated NO$_3^-$ ions [27].

A TEM micrograph of the Ni(II)–Cr(III) LDHs prepared at 483 K is shown in Fig. 3A. It is interesting to note that the size of the well-defined hexagonal platelets is much larger than L_{110} (Table 1), yet their electron diffraction pattern resembles that of monocrystalline particles (see inset in Fig. 3A); peak broadening by lattice strain cannot, however, be disregarded. The powder prepared at 413 K, on the other hand (Fig. 3B), is composed of irregular aggregates of small, ca. 10 nm in size, particles.

Table 1 summarizes the characteristics of the synthesized LDHs. The chromium-to-total-metal mole ratio in the Ni$_{1-x}$-Cr$_x$(OH)$_2$(CO$_3$)$_{x/2}$·nH$_2$O particles is slightly higher than that of the starting solution; x values from EDS agree, within experimental error, with those determined chemically. EDS analyses were performed on different spots of the specimens. The small standard deviations (σ) of the measurements indicate that the particles are highly uniform in chemical composition. The decrease of σ with increasing temperature, although slight, may reflect different degrees of ripening. Chemical analyses of the remaining supernatant solutions indicate that precipitation of Ni(II)–Cr(III) LDHs is nearly complete, irrespective of the ag-
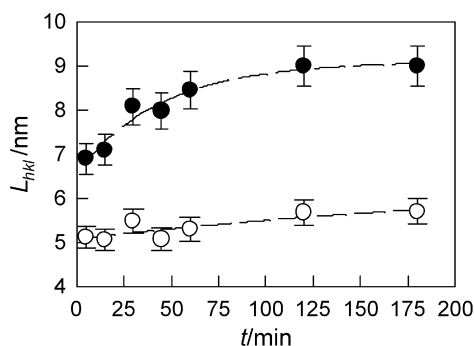
Fig. 4. Evolution of the crystallite size of Ni(II)–Cr(III) LDHs formed from $C_0 = 0.01$ M, $X_{Cr} = 0.36$, urea = 0.5 M solutions aged at 453 K: (●) L_{110}; (○) L_{003}.

Fig. 5. FTIR spectra of layered Ni(II)–Cr(III) hydroxides formed from Ni(NO$_3$)$_2$–Cr(NO$_3$)$_3$–urea solutions aged at 453 K for different times: (A) 5, (B) 30, (C) 60, and (D) 180 min. Initial solution composition: $C_0 = 0.01$ M; $X_{Cr} = 0.36$; urea = 0.5 M. The inset shows the whole spectrum of the solid formed after 5 min aging.

ing temperature; the fractions of dissolved Ni(II) and Cr(III) range between 3 and 5% and 0.5 and 1%, respectively.

The content of carbonate (Table 1) is nearly stoichiometric for the LDH prepared at 483 K and is substantially higher at the lower temperatures. The trend matches both the reduction of particle size (Fig. 3) and the decrease in the symmetry of the carbonate ions (Fig. 2). Since C_{2v} or C_s site symmetry relates to coordinated carbonate only [28], this parallelism indicates that the bands at 1480–1490, 1388, and 1067 cm^{-1} should be assigned to the ν_5, ν_1, and ν_2 vibration modes of carbonato *surface complexes* [29], in which CO$_3^{2-}$ ions replace the OH groups pending at the particle edges [30]. The presence of interlamellar HCO$_3^-$ ions could also explain the excess of carbonate, but, to the best of our knowledge, no bicarbonate-containing LDHs has yet been reported.

Recently, Kloprogge et al. [12] suggested that LDHs synthesized via the urea method intercalate (NH$_2$)COO$^-$ anions, an interlamellar species that, according to the authors, would account for the apparent C_{2v} character of the bands assigned to CO$_3^{2-}$. The absence of bands due to NH vibrations (2960–2850 cm^{-1}) in Fig. 2 (see also inset in Fig. 5 below) rules out the presence of (NH$_2$)COO$^-$ species in our solids. Thus, the C_{2v} character of the spectra shown here must be attributed to carbonato surface complexes. It worth stressing that (NH$_2$)COO$^-$ has not been identified as an intermediate of urea hydrolysis [13,31]. Furthermore, bands due to CO$_3^{2-}$ in the C_{2v} symmetry are not exclusive of LDHs synthesized via the urea method [23–26].

At 453 K, complete precipitation is attained within 5 min; the measured fractions of dissolved Ni(II) and Cr(III) are 4 and 1%, respectively, and remain constant throughout the aging of the systems ($C_0 = 0.01$ M; $X_{Cr} = 0.36$). Fig. 1E shows that, under these experimental conditions, formation of Ni(II)–Cr(III) LDH occurs as soon as precipitation takes place. Upon aging, the crystallites grow (Fig. 4). The increase of L_{003} is minor and nearly linear, whereas the growth along the xy plane is more pronounced. A similar trend was observed during the aging of freshly coprecipitated hydrotalcite [32].

FTIR spectra of the solids aged for different periods (Fig. 5) show that nitrate ions are rapidly exchanged for CO$_3^{2-}$. More importantly, they indicate that the amount of coordinated carbonate ions (C_s symmetry) decreases upon aging; the bands
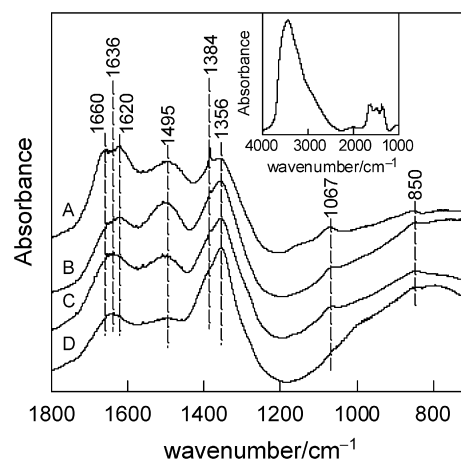
at 1660 and 1620 cm^{-1} (spectrum A) denote the presence of bidentated carbonate at very short times [28]. The evolution of the spectra indicates not only ripening, but, in terms of our previous assignment, also particle growth. None of the spectra, and especially spectrum A (see inset in Fig. 5), present features that would reveal the early precipitation of α-Ni(OH)$_2$.

4. Discussion

Formation of LDHs from aqueous solutions may proceed either by coprecipitation followed by dissolution and recrystallization or via homogeneous nucleation. The former mechanism is controlled by the rate of dissolution of the individual hydroxides, whereas the latter is determined by the ease of formation of heteronuclear hydroxo precursor complexes. Thus, the actual operating mechanism depends on the relative pace of these processes.

As a rule, Ni(II)–Cr(III) LDHs form via redissolution of *act*-Cr(OH)$_3$ (an assembly of hydrogen-bonded Cr(H$_2$O)$_3$(OH)$_3$ monomers [33]) and Ni(OH)$_2$ [5,15], which are two sluggish processes [34]. The reluctance of Ni(II)–Cr(III) LDHs to undergo homogeneous nucleation, which should involve the nucleophilic attack of, say, Cr(H$_2$O)$_5$OH^{2+} on Ni(H$_2$O)$_6^{2+}$, in a process where Ni^{2+} ions loosen water molecules from their first hydration shell, can be understood on the basis of the reported water exchange rate constants listed in Table 2. Comparison of $k_{Ni–H_2O}$ with the rate constant for the first protolysis of Cr(H$_2$O)$_6^{3+}$ ($k_{a1} = 1.4 \times 10^5$ s^{-1} [37]; subsequent protolysis steps are expected to be equally fast) indicates that the slower water-exchange kinetics of Ni(II) inhibits the formation of Ni(II)–Cr(III) heteronuclear hydroxo species, because the ensuing faster protolysis of Cr(H$_2$O)$_5$OH^{2+} leads to *act*-Cr(OH)$_3$.

From the data in Table 2, it may seem surprising that the urea method fails to produce Zn(II)–Cr(III) and other Cr(III)-containing LDHs under usual synthesis conditions (i.e., 350–370 K) [9]. However, hydrolysis is always coupled to the rate

Table 2
Hydrolytic properties of selected metal ions at 298 K

	Electron conf.	pK_1[a]	$p\beta_2$[a]	$p\beta_3$[a]	$k_{M–H_2O}$ (s^{-1})[b]
Ni^{2+}	Ar d^8	9.86	9.14		$2.7–3.6 \times 10^4$
Cr^{3+}	Ar d^3	4.0	5.7	8.3	$4.3–5.8 \times 10^{-7}$
Zn^{2+}	Ar d^{10}	8.96	7.96		$3.0–7.2 \times 10^7$
Al^{3+}	Ne	4.97	4.03	5.7	16

[a] K_1 is the first hydrolysis constant of the hexaaquo metal ions, and β_2 and β_3 are the equilibrium constants of the successive hydrolysis steps; they were taken from Ref. [35].
[b] From Ref. [36].

of base dosing, which is a critical variable in the definition of the prevailing mechanism. In fact, comparison of k_{a1} and $k_{Zn–H_2O}$ indicates that, at relatively high rates of base dosing, precipitation of *act*-Cr(OH)$_3$ should compete favorably with the homogeneous formation of Zn(II)–Cr(III) hydroxo precursors. It must be noticed that within the above-mentioned temperature range separate nucleation events usually take place [38,39]. The subsequent evolution of the coprecipitated hydroxides to form the final solid depends strongly on the reactivity of the involved metal ions; e.g., for labile ions, such as Cu^{2+} and Zn^{2+}, double basic carbonates form readily [38]. Thus, owing to the higher lability of Al^{3+} than of Cr^{3+} (Table 2), less stringent aging conditions are required for the preparation of Al(III)-containing LDHs via the urea method [9–12]. It should be recognized here that homogeneous nucleation of Zn(II)–Cr(III) LDHs takes place under the conditions provided by slow pH-titration experiments [40].

Since the water-exchange rate constant for Ni(H$_2$O)$_5$OH$^+$ is 2×10^5 s^{-1} [41], and must be larger for Ni(H$_2$O)$_4$(OH)$_2$ [36], the above rationale further suggests that heteronuclear Cr(III)–Ni(II) hydroxo complexes should form if simultaneous hydrolysis of Cr(H$_2$O)$_6^{3+}$ and Ni(H$_2$O)$_6^{2+}$ is realized, e.g., in an ideal pH-jump–pH-stat experiment. This situation, seldom attained under the usual synthesis conditions, can in principle be achieved under microwave-assisted hydrothermal ones. At 493 K, the half-life of urea is ca. 23 s [31]; hence, in excess urea, a very large driving force is soon attained. Our data suggest that this premise may have actually been fulfilled. The absence of structural (see Fig. 1E) and spectral features (see inset in Fig. 5) that would denote the early precipitation of α-Ni(OH)$_2$ supports the idea that Ni(II)–Cr(III) LDHs nucleate without the participation of intermediary solid phases. Patterns A and D in Fig. 1 also point in the same direction; the faster homogeneous nucleation renders better crystallized Ni(II)–Cr(III) LDHs.

According to density functional calculations [42], homogeneous nucleation of Ni(II)–Cr(III) LDHs should involve the edge-on condensation of planar hydroxo trimers, say, [Ni$_2$(μ_3-OH)(μ_2-OH)$_3$Cr(OH)$_y$(OH$_2$)$_{9-y}$]$^{(3-y)+}$ (see Fig. 6). Whether planar trimers or linear ones, as suggested by Roussel et al. [40], are the actual nuclei precursors, is an open question. The principle of *minimal structural change* [43], which establishes that precursors must bear close resemblance to the final octahedral ensemble, favors the former. In addition, the condensation of planar trimers, which is restricted to the xy-plane, is in line with the *periodic bond chain* approach [44,45].

As soon as the layers develop, they stack along the c axis (Fig. 4), giving rise to primary particles that aggregate to yield the final hexagonal platelets (cf. Table 1 and Fig. 3), in a process that involves the exchange of CO$_3^{2-}$ ions dangling at the crystallite edges by OH$^-$ (Fig. 5). Anions are known to play a major role during growth [46]. Ordered aggregation, which has been nicely documented earlier [47,48], is sketched in Fig. 6.
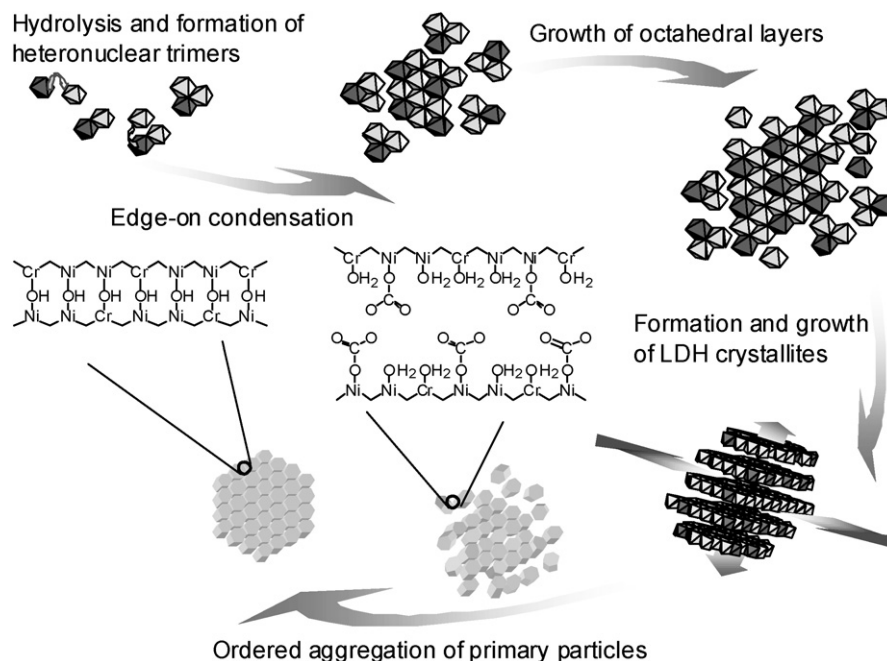

Fig. 6. Schematic representation of the homogeneous nucleation and growth of layered Ni(II)–Cr(III) double hydroxide particles. Darker octahedra represent Cr(H$_2$O)$_{6-n}$(OH)$_n^{(3-n)+}$ species; interlamellar anions are omitted for clarity.

5. Conclusions

The ease of LDH direct homogeneous nucleation depends heavily on the rate of base addition. Fast titration techniques are in this sense better than low-temperature homogeneous alkalization by urea hydrolysis. In this paper, it is shown that the combination of the latter procedure with high temperatures, achieved by microwave heating, is especially suited to obtaining well-crystallized LDHs in very short times, even when substitution robust ions, such as Cr(III) and Ni(II), are involved.

Acknowledgments

References

[1] F. Cavani, F. Trifiró, A. Vaccari, Catal. Today 11 (1991) 173.
[2] V. Rives, M.A. Ulibarri, Coord. Chem. Rev. 181 (1999) 61.
[3] A.I. Khan, D. O'Hare, J. Mater. Chem. 12 (2002) 3191.
[4] S. Miyata, A. Okada, Clays Clay Miner. 25 (1977) 14.
[5] O. Clause, M. Gazzano, F. Trifiró, A. Vaccari, L. Zatorski, Appl. Catal. 73 (1991) 217.
[6] S. Komarneni, Q.H. Li, R. Roy, J. Mater. Res. 11 (1996) 1866.
[7] S. Kannan, R.V. Jasra, J. Mater. Chem. 10 (2000) 2311.
[8] D. Tichit, A. Rolland, F. Prinetto, G. Fetter, M. de J. Martínez-Ortiz, M.A. Valenzuela, P. Bosche, J. Mater. Chem. 12 (2002) 3832.
[9] U. Costantino, F. Marmottini, M. Nocchetti, R. Vivani, Eur. J. Inorg. Chem. (1998) 1439.
[10] M. Ogawa, H. Kaiho, Langmuir 18 (2002) 4240.
[11] B. Mavis, M. Akinc, J. Power Sources 134 (2004) 308.
[12] J.T. Kloprogge, L. Hickey, R. Trujillano, M.J. Holgado, M.S. San Román, V. Rives, W.N. Martens, R.L. Frost, Cryst. Growth Des. 6 (2006) 1533.
[13] G.J. de A. A. Soler-Illia, M. Jobbágy, R.J. Candal, A.E. Regazzoni, M.A. Blesa, J. Dispersion Sci. Technol. 19 (1998) 207.
[14] R.S. Jayashree, P.V. Kamath, J. Power Sources 107 (2002) 120.
[15] F.M. Labajos, V. Rives, Inorg. Chem. 35 (1996) 5313.
[16] J.W. Boclair, P.S. Braterman, J. Jiang, S. Lou, F. Yarberry, Chem. Mater. 11 (1999) 303.
[17] A. de Roy, C. Forano, K. El Malki, J.-P. Besse, in: M.L. Occelli, H.E. Robson (Eds.), Synthesis of Microporous Materials, vol. II, Reinhold, New York, 1992, p. 108.
[18] L. Durand-Keklikian, I. Haq, E. Matijević, Colloids Surf. A 92 (1994) 267.
[19] F. Porta, S. Recchia, C. Bianchi, F. Confalonieri, G. Scari, Colloids Surf. A 155 (1999) 395.
[20] G.J. de A. A. Soler-Illia, M. Jobbágy, A.E. Regazzoni, M.A. Blesa, Chem. Mater. 11 (1999) 3140.
[21] S. Komarneni, Q.H. Li, K.M. Stefansson, R. Roy, J. Mater. Res. 8 (1993) 3176.
[22] K.A. Malinger, K. Laubernds, Y.-C. Son, S.L. Suib, Chem. Mater. 16 (2004) 4296.
[23] W.B. White, Am. Mineral. 56 (1971) 46.
[24] D.L. Bish, G.W. Brindley, Am. Mineral. 62 (1977) 46.
[25] F.M. Labajos, V. Rives, M.A. Ulibarri, Spectrosc. Lett. 24 (1991) 499.
[26] J. Pérez-Ramírez, G. Mul, F. Kapteijn, J.A. Moulijn, J. Mater. Chem. 11 (2001) 2529.
[27] M.J. Hernández-Moreno, M.A. Ulibarri, J.L. Rendon, C.J. Serna, Phys. Chem. Miner. 12 (1985) 34.
[28] K. Nakamoto, Infrared and Raman Spectra of Inorganic and Coordination Compounds, fourth ed., Wiley, New York, 1986.
[29] G. Lefèvre, Adv. Colloid Interface Sci. 107 (2004) 109.
[30] S.R. Randall, D.M. Sherman, K.V. Ragnarsdottir, Geochim. Cosmochim. Acta 65 (2001) 1015.
[31] J.W. Schoppelrei, M.L. Keike, X. Wang, M.T. Klein, T.B. Brill, J. Phys. Chem. 100 (1996) 14343.
[32] A. Ookubo, K. Ooi, H. Hayashi, Langmuir 9 (1993) 1418.
[33] R. Giovanoli, W. Stadelmann, W. Feitknecht, Helv. Chim. Acta 56 (1973) 839.
[34] M.A. Blesa, P.J. Morando, A.E. Regazzoni, Chemical Dissolution of Metal Oxides, CRC Press, Boca Raton, FL, USA, 1994, and references therein.
[35] C.F. Baes, P.E. Mesmer, The Hydrolysis of Cations, Wiley, New York, 1976.
[36] D.W. Margerum, G.R. Cayley, D.C. Weatherburn, G.K. Pagenkopf, in: A.E. Martell (Ed.), Coordination Chemistry, ACS Monograph 174, vol. 2, Am. Chem. Soc., Washington, DC, 1978, p. 1.
[37] L.D. Rich, D.L. Cole, E.M. Eyring, J. Phys. Chem. 73 (1969) 713.
[38] G.J. de A. A. Soler-Illia, R.J. Candal, A.E. Regazzoni, M.A. Blesa, Chem. Mater. 9 (1997) 184.
[39] M. Jobbágy, G.J. de A. A. Soler-Illia, A.E. Regazzoni, M.A. Blesa, Chem. Mater. 10 (1998) 1632.
[40] H. Roussel, V. Briois, E. Elkaim, A. de Roy, J.-P. Besse, J.-P. Jolivet, Chem. Mater. 13 (2001) 329.
[41] S. Funahashi, M. Tanaka, Inorg. Chem. 8 (1969) 2159.
[42] H. Sato, A. Morita, K. Ono, H. Nakano, N. Wakabayashi, A. Yamagishi, Langmuir 19 (2003) 7120.
[43] E. Boldyreva, in: J.A.K. Howard, F.H. Allen, G.P. Shields (Eds.), Implications of Molecular and Material Structure for New Technologies, NATO-ASI Series E, Kluwer, Dordretch, 1999, p. 151.
[44] P. Hartman, in: P. Hartman (Ed.), Crystal Growth: An Introduction, North-Holland, Amsterdam, 1973, p. 367.
[45] R. Rodríguez-Clemente, C.J. Serna, M. Ocaña, E. Matijević, J. Cryst. Growth 143 (1994) 277.
[46] E. Matijević, J. Colloid Interface Sci. 58 (1977) 374.
[47] E. Matijević, Chem. Mater. 5 (1993) 412.
[48] W.P. Hsu, L. Ronnquist, E. Matijević, Langmuir 4 (1988) 31.